

## HYDROTHERMAL AND METAMORPHIC BERTHIERINE FROM THE KIDD CREEK VOLCANOGENIC MASSIVE SULFIDE DEPOSIT, TIMMINS, ONTARIO

JOHN F. SLACK

*U.S. Geological Survey, National Center, Mail Stop 954, Reston, Virginia 22092, U.S.A.*

WEI-TEH JIANG AND DONALD R. PEACOR

*Department of Geological Sciences, University of Michigan, Ann Arbor, Michigan 48109, U.S.A.*

PATRICK M. OKITA\*

*U.S. Geological Survey, National Center, Mail Stop 954, Reston, Virginia 22092, U.S.A.*

### ABSTRACT

Berthierine, a 7 Å Fe–Al member of the serpentine group, occurs in the footwall stringer zone of the Archean Kidd Creek massive sulfide deposit, Ontario, associated with quartz, muscovite, chlorite, pyrite, sphalerite, chalcopyrite, and local tourmaline, cassiterite, and halloysite. Berthierine has been identified by the lack of 14 Å basal reflections on X-ray powder diffraction patterns, by its composition (electron-microprobe data), and by transmission electron microscopy (TEM). Petrographic and scanning electron microscopic (SEM) studies reveal different types of berthierine occurrences, including interlayers within and rims on deformed chlorite, intergrowths with muscovite and halloysite, and discrete coarse grains. TEM images show thick packets of berthierine and chlorite that are parallel or related by low-angle boundaries, and layer terminations of chlorite by berthierine; mixed-layer chlorite–berthierine also is observed, intergrown with Fe-rich chlorite and berthierine. End-member (Mg-free) berthierine is present in small domains in two samples. The Kidd Creek berthierine is chemically similar to berthierine from other localities, and to Fe-rich chlorite from a variety of geological settings. This is the first reported occurrence of berthierine from volcanogenic massive sulfide deposits. Textural relations suggest that most of the Kidd Creek berthierine formed as a primary hydrothermal mineral at relatively high temperatures (~350°C) in the footwall stringer zone, probably by the replacement of a pre-existing aluminous phase such as muscovite or chlorite. However, the intergrowth textures observed by SEM and TEM suggest that some of the berthierine originated by syn- or post-metamorphic replacement of chlorite. The difficulty of identifying berthierine by routine petrographic, X-ray, and electron-microprobe methods suggests that much of the Fe-rich chlorite described from modern and ancient massive sulfide deposits may instead be berthierine.

*Keywords:* berthierine, chlorite, volcanogenic sulfide deposit, transmission electron microscopy, electron-microprobe data, X-ray powder diffraction, Kidd Creek mine, Timmins, Ontario.

### SOMMAIRE

On trouve la berthierine, membre Fe–Al à 7 Å du groupe de la serpentine, dans la zone de minerai en veinules de la paroi inférieure du gîte archéen de sulfures massifs de Kidd Creek, en Ontario, en association avec quartz, muscovite, chlorite, pyrite, sphalérite, et chalcopryrite, avec présence locale de tourmaline, cassitérite et halloysite. On reconnaît la berthierine par l'absence d'une raie ayant une valeur  $d$  de 14 Å sur le cliché de diffraction X, par sa composition (données à la microsonde électronique), et par études au microscope électronique par transmission. Des études pétrographiques et au microscope électronique à balayage montrent que la berthierine se présente sous plus d'un aspect: elle forme une interstratification avec et une gaine sur la chlorite déformée, une intercroissance avec muscovite et halloysite, et des grains individuels relativement grossiers. Les images obtenues par transmission montrent d'épais amas de berthierine et de chlorite parallèles ou à faible angle d'incidence, et des feuillettes de chlorite ayant une terminaison de berthierine. Des assemblages mixtes de chlorite–berthierine sont aussi présents, en intercroissance avec chlorite ferrifère et berthierine. Le pôle ferrifère de la berthierine (sans Mg) est signalé en petits domaines dans deux échantillons. Du point de vue composition, la berthierine de Kidd Creek ressemble à celle d'autres endroits, et à la chlorite riche en Fe de plusieurs milieux géologiques. Nous signalons ici pour la première fois la présence de berthierine dans un gisement de sulfures massifs volcanogéniques. D'après les relations texturales, la plupart de la berthierine à Kidd Creek s'est formée comme minéral primaire à une température relativement élevée (~350°C) dans la zone à veinules de la paroi inférieure, probablement par remplacement d'un précurseur alumineux tel la muscovite ou la chlorite. Toutefois, les textures d'intercroissances observées par microscopie électronique à balayage et par transmission font penser qu'une partie de la berthierine a une origine par remplacement syn- ou post-métamorphique de la chlorite. La difficulté que nous avons éprouvée à identifier la berthierine par méthodes courantes de pétrographie, de diffraction X et d'analyse à la microsonde électronique nous incite à penser que la plupart des exemples de chlorite riche en fer cités dans la littérature sur les gîtes de sulfures massifs modernes ou anciens seraient plutôt de la berthierine. (Traduit par la Rédaction)

*Mots-clés:* berthierine, chlorite, gîte volcanogénique de sulfures massifs, microscopie électronique par transmission, données à la microsonde électronique, diffraction X, méthode des poudres, mine de Kidd Creek, Timmins, Ontario.

\*Present address: BHP-Utah International Inc., 200 Fairbrook Drive, Herndon, Virginia 22070, U.S.A.

## INTRODUCTION

Chlorite is one of the most abundant minerals in the alteration zones of volcanogenic massive sulfide deposits (e.g., Franklin *et al.* 1981); it typically occurs in veins with quartz, sulfides, and other minerals, and as replacements of sedimentary and volcanic host-rocks. In ancient metamorphosed deposits, chlorite may be the most common layer silicate, together with variable amounts of phengitic muscovite  $\pm$  paragonite; talc, stilpnomelane, and biotite generally are rare. In the pristine, unmetamorphosed alteration zones of the Miocene Kuroko deposits of Japan, layer-silicate assemblages are complex and include chlorite, illite, smectite, local talc, celadonite, and vermiculite, and rare chrysotile (Iijima 1974, Shirozu 1974, Utada *et al.* 1974, Shirozu *et al.* 1975). The alteration pipes of Cretaceous massive sulfide deposits on Cyprus, also unmetamorphosed, contain illite, chlorite, smectite, and rectorite (Lydon & Galley 1986, Richards *et al.* 1989). In this paper, we describe the occurrence of berthierine, an Fe–Al serpentine-type mineral, and berthierine–chlorite mixtures from the metamorphosed Kidd Creek massive sulfide deposit, of Archean age, and discuss the implications of these mixtures for interpreting the paragenesis of Fe–Al layer silicates in modern and ancient volcanogenic sulfide environments.

## IDENTIFICATION AND OCCURRENCE

*Geological setting*

The large Kidd Creek Cu–Zn–Pb–Ag deposit, north of Timmins, Ontario, consists of massive pyrite, chalcopyrite, sphalerite, pyrrhotite, and galena locally underlain by a chalcopyrite-rich stringer zone (Walker *et al.* 1975, Coad 1985). The ores are hosted by Archean volcanic rocks dated by U–Pb zircon methods at 2717 Ma (Nunes & Pyke 1981, Barrie & Davis 1990) and are believed to have formed on or near the sea floor synchronously with local volcanism and sedimentation. Multiple events related to postore deformation are evidenced by mine-scale faults and shear zones, strain fabrics in hand specimen and thin section, and U–Pb geochronological data (Walker *et al.* 1975, Brisbin *et al.* 1990, Barrie & Davis 1990). Regional metamorphism, which only reached lower greenschist grade, took place at approximately 2685 Ma (Percival & Krogh 1983) and was followed by a local metasomatic event in the mine area at about 2576 Ma (Maas *et al.* 1986).

*X-ray powder diffraction*

Slack & Coad (1989) recently described the textures and chemistry of Mg- and Fe-rich chlorite from the footwall stringer zone at Kidd Creek and suggested that these two compositional types of chlorite formed during separate hydrothermal events. The chlorite was identi-

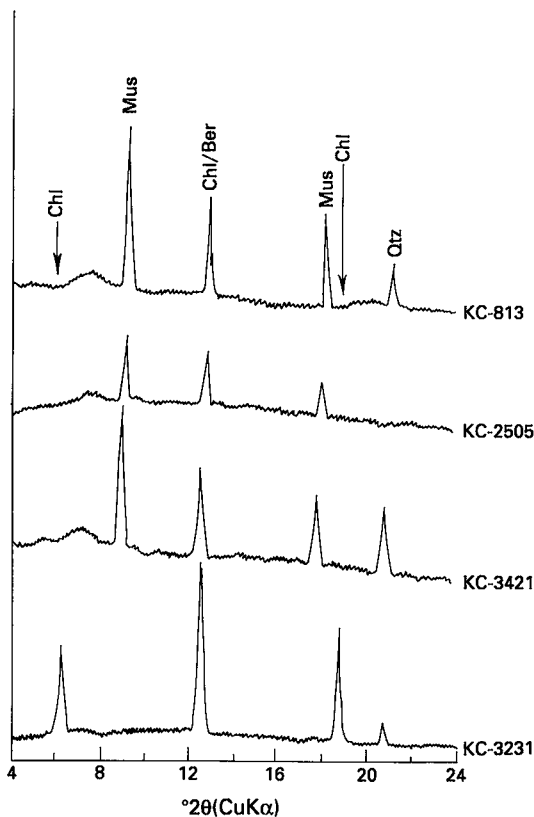


FIG. 1. X-ray powder-diffraction patterns (CuK $\alpha$  radiation) for mineral separates of layer silicates from the footwall stringer zone (north orebody) of the Kidd Creek mine. Patterns for samples KC-813, KC-2505, and KC-3421 lack the diagnostic  $\sim$ 14 Å (6.3°2 $\theta$ ) and  $\sim$ 4.7 Å (18.8°2 $\theta$ ) peaks of true chlorite (chl) and consist mainly (or wholly) of berthierine (ber) mixed with muscovite (mus)  $\pm$  quartz (qtz); small peaks at 7.0–7.5°2 $\theta$  are instrumental artifacts. Compare pattern for sample KC-3231 (bottom) that contains only 14 Å chlorite. All patterns were acquired on air-dried and untreated samples.

fied (by JFS) on the basis of optical features and results of electron-microprobe analyses. Identification of the Fe-rich chlorite is in error, however, as shown by X-ray powder-diffraction (XRD) patterns of mineral separates of layer silicates from several samples (Fig. 1). The Fe-rich silicate lacks the diagnostic 14 Å reflection of chlorite, and therefore is berthierine, an Fe–Al member of the serpentine group (e.g., Brindley 1982, Bailey 1988). The Fe-rich chlorite (“daphnite”) described by Slack & Coad (1989, Table 2, Fig. 12) consists largely or wholly of berthierine, including that in samples KC-813, KC-2505, KC-3421, and KC-3482. An XRD study of layer silicate separates from the other Kidd Creek samples (e.g., KC-3231, Fig. 1) shows prominent

TABLE 1. X-RAY POWDER-DIFFRACTION DATA FOR BERTHIERINE

hkl (mono)	hkl (hck)	Ayrshire* d-calc	Corby <sup>†</sup> d-calc	KC-813 d-calc	KC-3421 d-calc
001	010	7.05	7.12	7.09	7.08
020	100	4.67	4.68		
110		4.58			
111		4.28	4.30	4.26	4.26
021	101	3.90	3.93		
002	002	3.52	3.55	3.55	3.53
022		2.80	2.84	2.84	
201	110	2.68	2.71	2.65	2.71
210	111	2.52	2.53	2.53	
131		2.40		2.45	2.46
212		2.34		2.36	
132		2.27		2.28	2.28
222	112	2.14	2.15	2.22	2.13
132		2.01		2.08	2.00
133		1.894		1.943	1.869
311	004	1.769	1.779	1.775	1.818
233		1.700		1.728	
060	300	1.555	1.563		1.563

\*PDF card 7-315. Berthierine from Ayrshire, UK (Brindley 1951)

<sup>†</sup>PDF card 31-618. Berthierine from Corby, UK (Brindley & Youell 1953)

14 Å basal reflections; thus these do contain chlorite. X-ray data acquired for samples KC-813 and KC-3421 (Table 1) yield similar *d*-values to those reported for berthierine from Ayrshire, Scotland (Brindley 1951) and Corby, England (Brindley & Youell 1953).

Formerly called septechlorite (Nelson & Roy 1958), and (incorrectly) chamosite and 7 Å chamosite, berthierine is an Fe-rich aluminous trioctahedral 7 Å layer silicate with a 1:1 structure similar to that of lizardite (Bailey 1988). Berthierine is difficult to recognize by normal XRD methods because the critical identifying feature, the absence of a 14 Å basal reflection, is commonly masked by a peak due to admixed chlorite (*e.g.*, Brindley 1982); conventional XRD studies can document the presence of berthierine only in samples that lack chlorite. Berthierine associated with a small amount of Mg-Fe-rich chlorite can be misidentified as Fe-rich chlorite, because Fe-rich chlorite has a very strong reflection at about 7 Å relative to its ~14 Å reflection (Brindley 1982). Mixed layering of berthierine and chlorite may be suggested by broader and weaker, odd-ordered 00*l* reflections, compared to those of pure chlorite (Dean 1983, Ahn & Peacor 1985). Possible minor (<10%) interstratified Fe-Mg-rich chlorite cannot be detected by XRD, however, because of the weak nature of the odd-order reflections (Reynolds 1988). The Kidd Creek samples that lack a 14 Å basal reflection (Fig. 1) thus consist either entirely of berthierine, or of berthierine and minor interlayered chlorite not resolvable by XRD methods.

#### Petrography and scanning electron microscopy

Berthierine from the Kidd Creek mine forms anhedral grains and subhedral crystals associated with quartz, muscovite, chlorite, pyrite, sphalerite, chalcopyrite, and local tourmaline, cassiterite, and halloysite. Typical

grain-sizes are 10–50 µm, although some large crystals that appear prismatic in cross section (normal to {001}) in samples KC-3421 and KC-3482 are as much as 100–200 µm long. Berthierine grains commonly are pleochroic from colorless to pale green or from pale green to medium green, and most have higher birefringence than chlorite-group minerals (*e.g.*, Hey 1954, Albee 1962), producing yellow to orange (rarely purple) first-order interference colors ( $n_{\gamma}-n_{\alpha} \approx 0.018$ ). However, the berthierine grains in several samples have lower birefringence and superficially resemble chlorite, thus leading to misidentification based on petrographic criteria alone.

Berthierine grains in sample KC-3421 are locally associated with a white clay mineral. X-ray data obtained with a Debye-Scherrer camera (H.T. Evans, Jr., USGS, pers. commun., 1991) indicate that this clay is halloysite-7 Å, with possibly a trace of halloysite-10 Å. Electron-microprobe analyses, using a defocused beam, show 45–46% SiO<sub>2</sub>, 36–37% Al<sub>2</sub>O<sub>3</sub>, 0.1–0.7% FeO, and anhydrous oxide totals of 83–84%, consistent with the presence of halloysite. The halloysite forms irregular zones (Fig. 2A) commonly 0.5–1.0 mm in diameter within massive sphalerite, and intergrowths with muscovite, quartz, and sparse fluorite; berthierine occurs along the margins of some halloysite zones (Fig. 2B). One large zone of halloysite fills what appears to be a former aggregate of euhedral flakes of muscovite (or another phyllosilicate) in sphalerite (not shown), suggesting a paragenesis of early muscovite (?) followed by a later stage involving pseudomorphous replacement by halloysite. Inclusions of muscovite in some of the halloysite zones display embayed, corroded edges, whereas others have smooth boundaries; similar relations exist between sphalerite and layer silicates. The halloysite is interpreted as a late hydrothermal phase, and not a product of supergene alteration or weathering, based on the lack of fractures in this sample and the absence of any secondary minerals diagnostic of oxidation or weathering (*e.g.*, hematite, covellite, goethite). Halloysite has been identified in some of the Miocene Kuroko deposits of Japan (*e.g.*, Nurukawa) and recently in the modern Kuroko-type Jade deposit actively forming in the Okinawa Trough (Marumo 1991). Stanton (1983) reported possible halloysite from the Archean Geco massive sulfide deposit in Ontario, but without supporting XRD evidence. The occurrence in the Kidd Creek deposit appears to be the first example of hypogene halloysite documented in Precambrian rocks.

Berthierine commonly displays complex intergrowths with both muscovite and chlorite. Euhedral berthierine blades enclosed within sphalerite in sample KC-3421 locally show embayed contacts with muscovite (Fig. 2C) that suggest replacement of muscovite (or a pre-existing phyllosilicate) by berthierine. However, other areas of this sample and areas within sample KC-813 (Fig. 2D) have "equilibrium" textures that imply contemporaneous formation of muscovite and

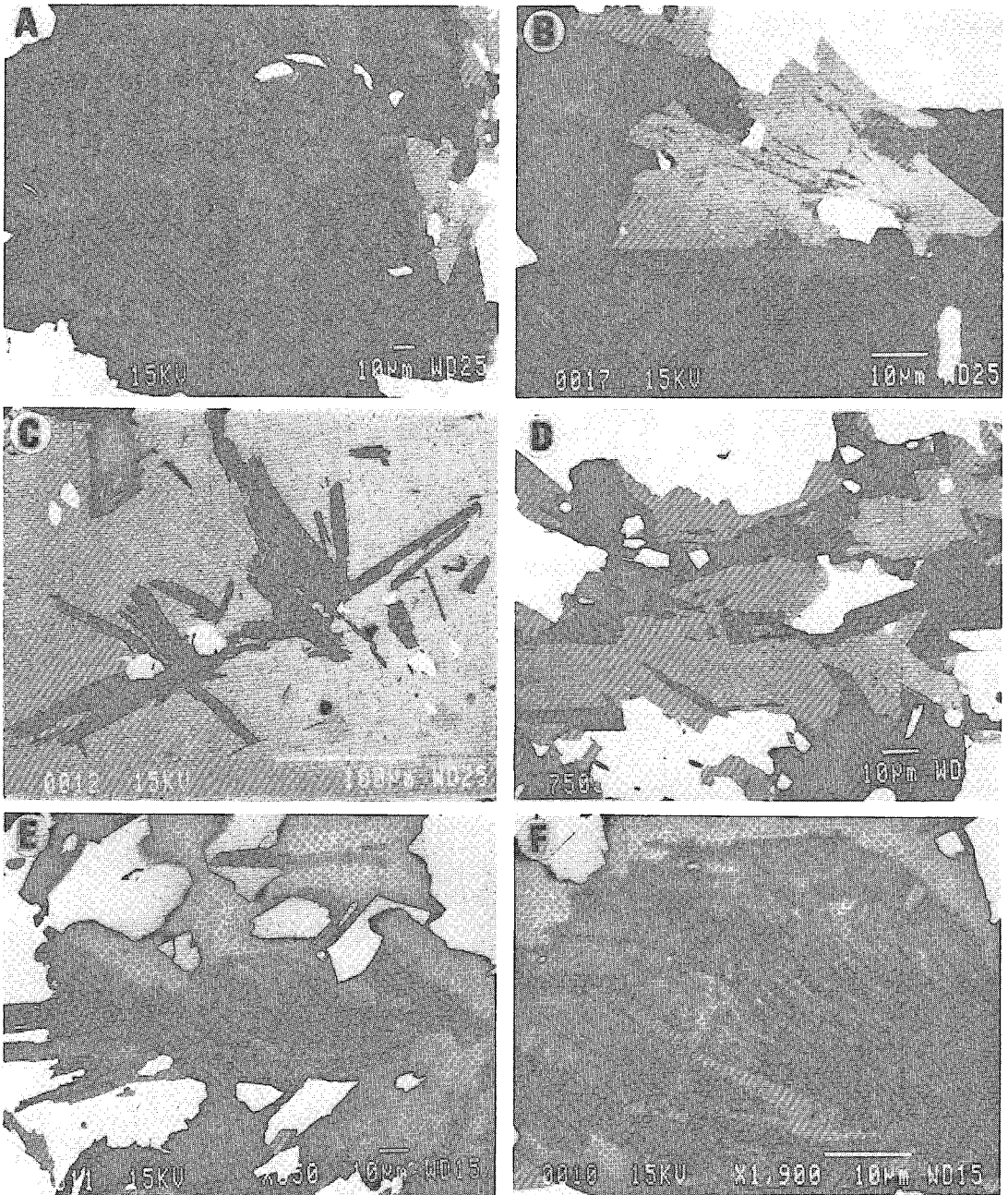


FIG. 2. SEM back-scattered electron images of samples from the footwall stringer zone. A. Intergrowth of halloysite (dark grey) with muscovite (medium grey) and berthierine (pale grey) along right edge, surrounded by sphalerite (white); black areas are open pits (sample KC-3421). B. Detail of A showing euhedral berthierine (pale grey) in contact with muscovite (medium grey) and halloysite (dark grey) and associated with sphalerite in white (sample KC-3421). C. Massive sphalerite (pale grey) enclosing prismatic grains of berthierine (medium grey) apparently replacing muscovite (dark grey); small white grains are cassiterite (sample KC-3421). D. Grains of berthierine (pale grey) intergrown with and surrounded by muscovite (medium grey), and associated with quartz (dark grey); sphalerite is white (sample KC-813). E. Elongate composite grain of berthierine (pale grey) and Fe-Mg chlorite (medium grey); muscovite is black and surrounding chalcopyrite is white (sample KC-2505). F. Detail of E showing alternating lamellae of finely intergrown berthierine (pale grey) and Fe-Mg chlorite (medium grey), and rims of berthierine on chlorite; black areas are cracks and voids between mineral lamellae (sample KC-2505); see Table 2 for results of electron microprobe analyses of the chlorite (no. 2505F1) and berthierine (no. 2505F2) in this grain.

berthierine (or its precursor). Berthierine in sample KC-3421 exhibits embayed and corroded edges and seems to be partially replaced by the associated halloysite (Fig. 2B).

Figure 2E shows a composite grain of berthierine and chlorite partly surrounded by muscovite in chalcopyrite-rich sample KC-2505 from the core of the stringer zone (see Slack & Coad 1989, Fig. 2). This grain is clearly deformed, consistent with the presence in the same sample of microscopic chevron folds defined by deformed muscovite, chlorite, and sulfides. Most of the borders of the composite grain (Fig. 2E) contain a thin (<5  $\mu\text{m}$ ) rim of nearly end-member (Mg-free) berthierine, whereas the interior has very fine lamellae of berthierine <1  $\mu\text{m}$  in diameter (Fig. 2F). The deformation may have caused bending and gliding of chlorite layers, resulting in separation of the layers and formation of the elongate lens-shaped voids. Packets of berthierine oriented parallel to the voids also have a similar lens-like shape, and several of the voids contain a berthierine rim, although some berthierine lamellae have different orientations and are not associated with voids. One interpretation of these features is that the chlorite and berthierine represent primary hydrothermal precipitates that were deformed together, producing the paragenetically late, lens-shaped voids. Alternatively, berthierine may have formed by filling of deformation-related voids or by the replacement of previously deformed chlorite. Similar lens-shaped replacements of deformed phyllosilicates have been widely reported in low-grade metamorphosed and hydrothermally altered rocks (Craig *et al.* 1982, van der Pluijm & Kaars-Sijpesteijn 1984, Gregg 1986, Ahn & Peacor 1987, Bons 1988).

#### Transmission electron microscopy

Part of a thin section of sample KC-2505 was prepared for transmission electron microscopy (TEM) following optical and SEM studies. A 3-mm-diameter area adhering to an aluminum washer was detached from the thin section and a Cu grid backing was attached to one side to prevent the possible loss of thin edges due to differential thinning and expansion-contraction rates of layer silicates and sulfides during Ar ion-beam milling. A Philips CM12 scanning transmission electron microscope<sup>1</sup> coupled with a low-angle Kevex Quantum detector for EDS analysis was used for the TEM observations at the University of Michigan. The 00l reflections up to the third order (chlorite) were selected to produce one-dimensional lattice fringe images.

Chlorite in sample KC-2505 was observed to consist of three principal textural types, including (1) discrete,

large crystals of Fe-Mg-rich chlorite, (2) single layers or very thin packets of layers interstratified with berthierine (*i.e.*, mixed-layer chlorite-berthierine), and (3) crystals of relatively Fe-rich chlorite (designated hereafter as Fe-chlorite) that are intimately intergrown with mixed-layer chlorite-berthierine. In addition to the mixed layering, discrete, thick packets of berthierine intergrown with chlorite also are present, analogous to the berthierine lamellae shown in Figure 2F.

Figure 3 shows typical relations between berthierine and the three different types of chlorite. Each layer silicate forms relatively thick, well-defined, discrete packets that are parallel or subparallel, with berthierine and mixed-layer chlorite-berthierine occurring preferentially at the boundaries of chlorite crystals. The individual packets of chlorite seem similar to those of phyllosilicates affected by metamorphic processes that locally approach an equilibrium state, with an absence of the heterogeneous features (*e.g.*, mixed layering) that characterize textures formed at very low temperatures (*e.g.*, Ahn & Peacor 1985). However, packets of Fe-chlorite, Fe-Mg-rich chlorite, and chlorite in mixed-layer berthierine-chlorite occur immediately adjacent to one another, a feature that clearly indicates nonequilibrium conditions.

Several types of deformation features are observed. In the middle-right part of Figure 3 is a pale grey area with an arrowhead shape that separates Fe-Mg-rich chlorite that presumably was once continuous, as the outlines on both sides of the arrowhead-shaped area are nearly identical. We are unable to identify the material within this arrowhead-shaped area, but it appears to be a noncrystalline phase containing Al, Si, K, Mg, Fe, S, Cu, and Cl, as suggested by EDS spectra. The packet of Fe-Mg chlorite that is dissected by the arrowhead-

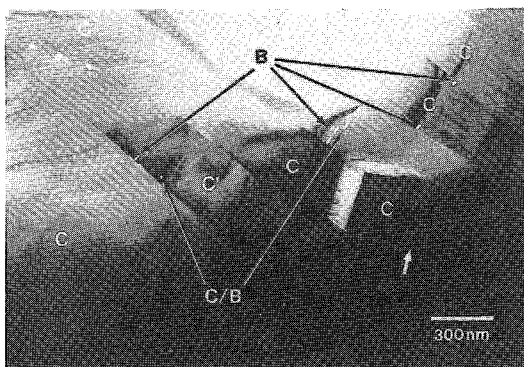


Fig. 3. Transmission electron microscopic image of sample KC-2505 showing intergrowths of berthierine with Fe-Mg chlorite (C), Fe-chlorite (C'), and mixed-layer chlorite-berthierine (C/B). The pale grey arrowhead-shaped area in the middle-right is a noncrystalline phase (see text). The white arrow indicates a kinked area in chlorite.

<sup>1</sup>Any use of trade, product, or firm names is for descriptive purposes only and does not imply endorsement by the U.S. Government.

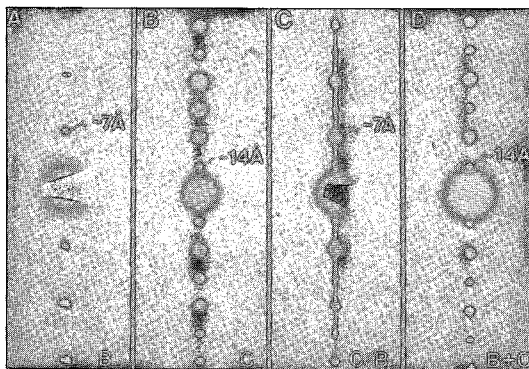


FIG. 4. Selected-area electron-diffraction patterns of areas in Figure 3 showing  $00l$  reflections of A) berthierine, B) Fe–Mg chlorite, C) mixed-layer chlorite–berthierine, and D) chlorite + berthierine. The beam stopper was used for A and C.

shaped area has a prominent kink (indicated by the white arrow). Thicknesses of the packets next to that of the kinked packet vary along the packet, consistent with

gliding along boundaries with a component normal to the image. Variations in contrast occur within some of the chlorite and berthierine packets, apparently reflecting strain. The strain contrast at the crystal boundary in the middle-left part of the image suggests that there is a lattice misfit, in agreement with an origin due to gliding along partially coherent interfaces, as is normally the case in gliding facilitated by dislocations. Such deformation features have not been observed in berthierine and mixed-layer chlorite–berthierine regions, which implies that some of the berthierine is probably syn- or post-deformation in origin, replacing deformed chlorite or voids created during deformation.

Selected-area electron-diffraction (SAED) patterns were obtained from different areas of Figure 3. The SAED patterns are consistent with the presence of berthierine (7 Å periodicity, Fig. 4A), chlorite (14 Å periodicity, Fig. 4B), and mixed-layer chlorite–berthierine (relatively weak, diffuse odd-order and strong, sharp even-order  $00l$  reflections where  $d(001) \approx 14$  Å, Fig. 4C). The continuous streak along  $c^*$  in Figure 4C suggests that the 14 Å (chlorite) and 7 Å (berthierine) layers are randomly interstratified in the mixed-layer areas. Like the interpretive problems of XRD patterns

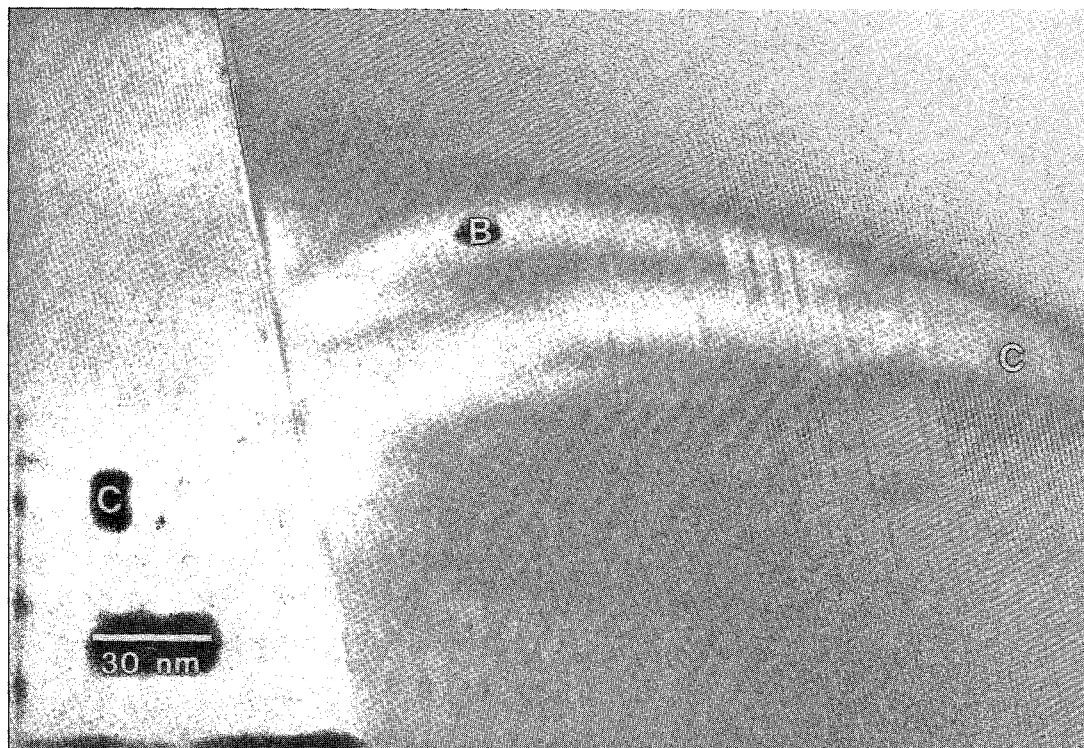


FIG. 5. Lattice-fringe image of intergrown berthierine (B), Fe–Mg chlorite (C), and mixed-layer chlorite–berthierine (C/B) in sample KC-2505. Layers showing  $\sim 7$  Å (narrow fringes) and  $\sim 14$  Å (wide fringes) periodicities are berthierine and chlorite, respectively. Layer terminations and complex mixed layering between chlorite and berthierine are present in the middle right.

discussed above, it is difficult to differentiate  $00l$  reflections of discrete berthierine + discrete chlorite (Fig. 4D) from those of only discrete chlorite (Fig. 4B).

Packets of berthierine and mixed-layer chlorite-berthierine are locally parallel or subparallel to adjacent packets of Fe-Mg chlorite (Fig. 5). Individual 14 Å layers are present within the berthierine packet, and discontinuities between 14 Å and 7 Å layers are present in the mixed-layer area. Such discontinuities may be due to variation in the inclination of  $c^*$  along the layers or to variations in crystal thickness (Amouric *et al.* 1988, Jahren & Aagaard 1989). However, in this case they appear to represent true interfaces because images that were obtained at different conditions of focus all display the same features.

Figure 6 shows alternating thick packets of berthierine and Fe-Mg chlorite layers that are parallel or related by low-angle boundaries. Such textures are analogous to those observed in many occurrences of phyllosilicate intergrowths that formed during prograde metamorphism (*e.g.*, Franceschelli *et al.* 1986, Frey 1987, Jiang *et al.* 1990). The variation in contrast along the layers in the upper left reflects strain, presumably due to shear

stress (Bons *et al.* 1990). The berthierine and chlorite packets in the lower part of the image seem to be unaffected. The slight variations in contrast on the right are principally due to decreasing thickness of the specimen toward the thin edges. Mixed layering and interstratification of packets of two phyllosilicate phases are common in replacement reactions of one phyllosilicate by the other (*e.g.*, Banfield & Eggleton 1988, Jiang & Peacor 1991), although they also may occur without phase transitions.

An electron-diffraction pattern of berthierine (Fig. 7A) shows a highly disordered sequence of stacking, as suggested by the strong streaks in the non- $00l$  reflection rows with  $k \neq 3n$ . The presence of very weak streaks and 14 Å reflections suggests that there is a minor component of chlorite interstratified with the berthierine. Disordered sequences of stacking are common in phyllosilicates that formed during diagenesis or very low-grade metamorphism (Kisch 1983, 1987). Such disordered sequences transform to ordered sequences during prograde metamorphism before conditions of the lower greenschist facies are attained. Coexisting muscovite, having a nearly end-member composition, with only

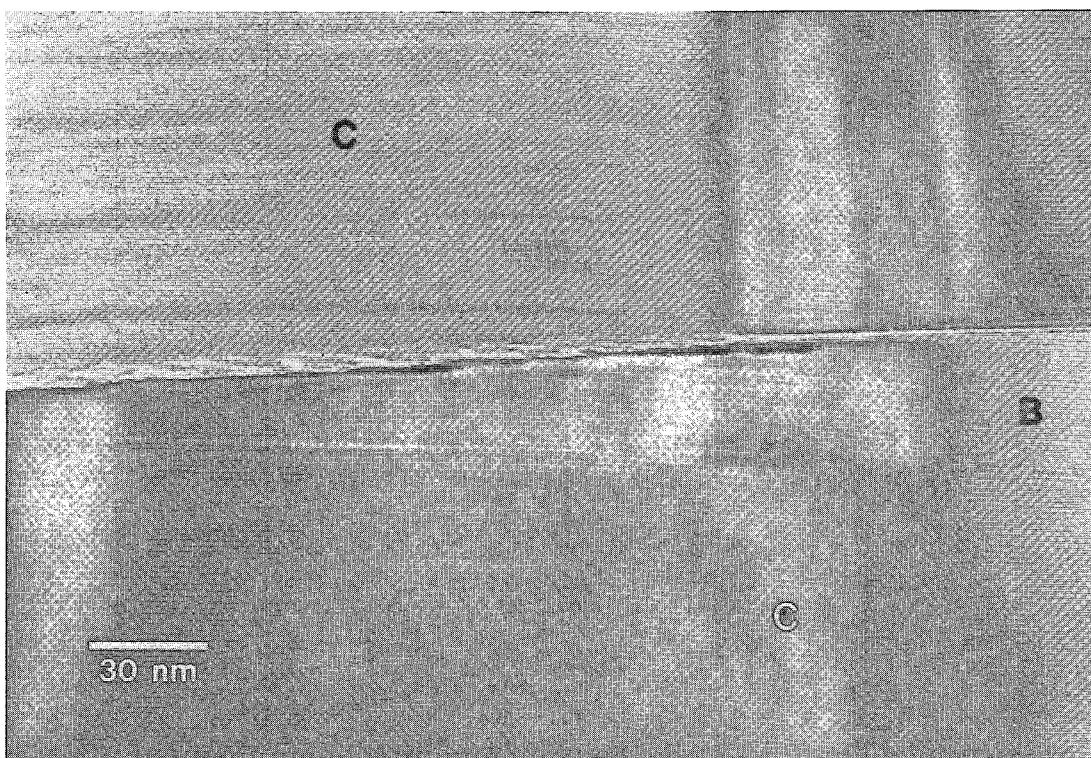


FIG. 6. Lattice-fringe image of sample KC-2505 showing alternating packets of berthierine (B) and Fe-Mg chlorite (C) that are parallel or related by low-angle boundaries.

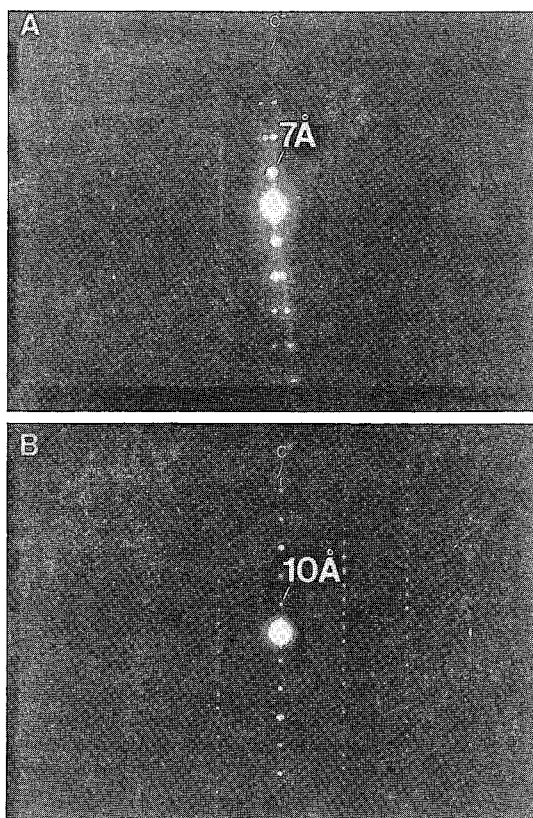


FIG. 7. Electron-diffraction patterns of berthierine in sample KC-2505 showing continuous streaking along  $c^*$  in  $OkI$  or  $hhl$  rows, suggesting a highly disordered stacking sequence (A), and the  $[110]$  or  $[\bar{1}\bar{1}0]$  zone of muscovite with  $20 \text{ \AA}$  periodicity in  $hhl$  or  $\bar{h}\bar{h}l$  rows, implying a two-layer polytype (B).

minor Fe and Mg, invariably occurs as a two-layer polytype, giving a  $20 \text{ \AA}$  periodicity in non- $00l$  reflection rows with  $k \neq 3n$  of SAED patterns (Fig. 7B) and with different contrast in alternate  $001$  fringes. The muscovite forms either discrete, large packets of layers, or small packets of layers enclosed within other phases; mixed layering between muscovite and other phases is not observed. All of these features in muscovite are consistent with equilibration of dioctahedral phyllosilicates under greenschist-facies conditions.

#### MINERAL CHEMISTRY

Slack & Coad (1989) reported on the results of detailed electron-microprobe analyses of Mg- and Fe-rich chlorite from Kidd Creek, the latter now recognized as berthierine. Selected compositions from that study,

together with more recent microprobe data (using the same methods and standards), are presented in Table 2. The berthierine contains nearly equal amounts of  $\text{SiO}_2$  and  $\text{Al}_2\text{O}_3$ , and most samples have little or no Na, Ca, or K. Many grains contain  $<1 \text{ wt\%}$  MgO, and several compositions from samples KC-813 and KC-3482 lack detectable MgO, thus documenting the occurrence of end-member berthierine (e.g., no. 813F, Table 2). Grains enclosed in sphalerite in sample KC-3421 have as much as  $2 \text{ wt\%}$  ZnO that indicate a small component of fraipontite, the zinc analog of berthierine (Fransolet & Bourguignon 1975). The minor amounts of Na, Ca, and K found locally in berthierine from samples KC-813 and KC-3421 suggest the presence of finely interlayered smectite or perhaps interlayered micas such as paragonite, muscovite, or margarite. Normalizations on the basis of an ideal chlorite anion formula ( $20 \text{ O} + 16 \text{ OH}$ ) reveal that  $^{\text{VI}}\text{Al}$  significantly exceeds  $^{\text{IV}}\text{Al}$  in all samples, in contrast with ideal end-member berthierine  $[(\text{Fe}_8\text{Al}_4)(\text{Si}_4\text{Al}_4)\text{O}_{20}(\text{OH})_{16}]$  for which  $^{\text{VI}}\text{Al} = ^{\text{IV}}\text{Al}$ . The excess  $^{\text{VI}}\text{Al}$  in the Kidd Creek samples may be related to the presence of intergrown Si-rich phases such as quartz, pyrophyllite, or talc, or to interlayering with a di, trioctahedral chlorite such as sudoite (e.g., Bailey & Lister 1989, Shau *et al.* 1990), with both the trioctahedral chlorite and berthierine. Sudoite has been identified in the alteration zones of several of the unmetamorphosed Kuroko deposits of Japan (Tsukahara 1964, Hayashi & Oinuma 1964) and the metamorphosed Geco massive sulfide deposit, Ontario (Stanton 1984). It is also possible that the excess  $^{\text{VI}}\text{Al}$  reflects vacancies in the octahedral sites (Foster 1962), which are common in berthierine (Brindley 1982) and some chlorite (e.g., Curtis *et al.* 1985).

Qualitative EDS and analytical electron microscopy (AEM) analyses have been acquired on sample KC-2505. The EDS analyses suggest that most of the berthierine crystals are more Fe-rich than coexisting chlorite, although very Fe-rich chlorite (*i.e.*, daphnite) is present locally (Fig. 3). Ahn & Peacor (1985) and Jahren & Aagaard (1989) have demonstrated that berthierine is generally more Fe-rich than chlorite, but that overlaps in Fe-Mg contents occur. The AEM analyses, carried out on materials defined as pure by TEM observation, are consistent with this relation. Extreme caution, therefore, must be used in the identification of Fe-rich chlorite, especially the aluminous varieties.

Figure 8 shows the average compositions of Kidd Creek berthierine and chlorite compared to the compositional fields for berthierine and chlorite from other localities. This diagram illustrates the overall chemical similarity between berthierine and chlorite, and the difficulty of distinguishing them on the basis of electron-microprobe data alone. Compositions of the Kidd Creek berthierine and chlorite all plot within the field of berthierine reported by Brindley (1982), Iijima & Matsumoto (1982), Bhattacharyya (1983), and Velde (1989), and also within the compositional fields of

TABLE 2. REPRESENTATIVE COMPOSITIONS OF BERTHIERINE AND CHLORITE

	813D	813E	813F	2505F1	2505F2	3421B	3482A	HIRAM	KURSK	CORBY	USSR
SiO <sub>2</sub> wt%	22.04	22.62	21.99	23.03	22.31	21.96	22.83	22.87	21.26	22.81	22.40
Al <sub>2</sub> O <sub>3</sub>	23.01	23.05	22.21	23.15	23.51	23.31	23.38	23.24	23.61	23.12	23.34
TiO <sub>2</sub>	0.07	0.05	0.03	0.05	0.04	0.01	0.03	n.a.	n.d.	n.a.	n.d.
FeO	42.70	41.37	42.99	33.31	41.07	41.94	36.77	40.15	39.19	39.66	39.63
MnO	0.26	0.22	0.16	0.13	0.13	0.27	0.14	n.a.	n.d.	n.a.	1.69
MgO	1.13	0.98	0.00	7.13	1.31	1.23	5.19	1.77	2.92	2.72	2.01
ZnO	n.a.	n.a.	n.a.	n.a.	n.a.	1.03	n.a.	n.a.	n.a.	n.a.	0.66
CaO	0.02	0.10	0.02	0.03	0.04	0.00	0.01	0.09	n.d.	n.a.	n.d.
Na <sub>2</sub> O	0.08	0.25	0.06	0.08	0.04	0.01	0.02	0.00	n.d.	n.a.	n.d.
K <sub>2</sub> O	0.04	0.51	0.08	0.19	0.06	0.02	0.00	0.00	n.d.	n.a.	0.29
Total	89.35	89.15	87.54	87.10	86.51	89.78	88.37	88.12	86.98	88.37	90.02

## Structural formulae on the basis of 28 oxygens

Si	5.034	5.150	5.153	5.123	5.087	5.000	5.086	5.198	4.904	5.162	5.045
Al <sup>IV</sup>	2.966	2.850	2.847	2.877	2.913	3.000	2.914	2.802	3.096	2.838	2.955
Al <sup>VI</sup>	3.227	3.336	3.286	3.193	3.406	3.250	3.225	3.422	3.324	3.331	3.243
Ti	0.012	0.008	0.006	0.008	0.007	0.001	0.006	0.005	0.000	0.000	0.000
Fe	8.155	7.876	8.424	6.196	7.834	7.980	6.852	7.632	7.559	7.506	7.465
Mn	0.050	0.043	0.033	0.027	0.025	0.026	0.026	0.000	0.000	0.000	0.322
Mg	0.386	0.334	0.000	2.363	0.446	0.418	1.724	0.600	1.004	0.917	0.675
Zn	0.000	0.000	0.000	0.000	0.000	0.172	0.000	0.000	0.000	0.000	0.110
Ca	0.004	0.023	0.004	0.008	0.011	0.000	0.003	0.022	0.000	0.000	0.000
Na	0.037	0.108	0.025	0.033	0.017	0.006	0.008	0.000	0.000	0.000	0.000
K	0.011	0.149	0.022	0.052	0.017	0.005	0.001	0.000	0.000	0.000	0.083
Total	19.882	19.877	19.800	19.880	19.763	19.884	19.845	19.681	19.887	19.754	19.898
Oct Vacancy	0.170	0.403	0.251	0.213	0.282	0.127	0.167	0.341	0.113	0.246	0.185
Fe/(Fe+Mg)	0.955	0.959	1.000	0.724	0.950	0.964	0.799	0.927	0.883	0.891	0.917
Mg/Fe	0.047	0.042	0.000	0.381	0.057	0.052	0.252	0.079	0.133	0.122	0.090

Notes: Total iron as FeO; n.a. = not analyzed or not reported; n.d. = not detected.

813D: berthierine associated with tourmaline, pyrite, minor sphalerite and quartz, and traces of sericite (from Slack & Coad 1989, Table 2); 813E: berthierine associated with quartz, sphalerite, pyrite, tourmaline, and minor sericite; 813F: berthierine associated with pyrite, quartz, sphalerite, and minor sericite; 2505F1: chlorite intergrown with berthierine and associated with sericite, chalcocopyrite, and minor quartz (see Fig. 2x); 2505F2: berthierine intergrown with chlorite and associated with sericite, chalcocopyrite, and minor quartz (see Fig. 2x); 3421B: berthierine associated with sericite, sphalerite, and minor chalcocopyrite and cassiterite (see Fig. 2x); 3482A: berthierine associated with tourmaline, quartz, pyrite, sphalerite, and minor sericite (from Slack & Coad 1989, Table 2); HIRAM: K-type berthierine of Iijima & Matsumoto (1982, Table 4) in Triassic fireclay beds from Hiramatsu area, Japan; KURSK: berthierine in bauxite deposits from Kursk, USSR (Yershova et al. 1976); CORBY: berthierine in Jurassic ironstone from Corby, Northamptonshire, UK (Brindley & Youell 1953); USSR: berthierine ± chlorite in Ag-Pb-Zn quartz vein, USSR (Rusina et al. 1987).

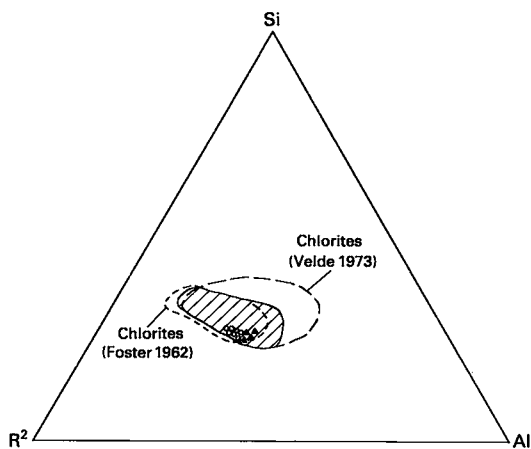


FIG. 8. Cation plot of average microprobe compositions of chlorite (open circles) and berthierine (solid triangles) at Kidd Creek compared to the compositional fields of chlorites compiled by Foster (1962) and Velde (1973) and the field of berthierines (hatched) from Brindley (1982), Iijima & Matsumoto (1982), Bhattacharyya (1983), and Velde (1989).  $R^2 = Fe^{2+} + Mg + Mn + Zn$ .

chlorite compiled by Foster (1962) and Velde (1973). However, the berthierine and chlorite from Kidd Creek differ slightly in relative proportions of Al and  $R^{2+}$  ( $Fe^{2+} + Mg + Mn + Zn$ ) cations. The Kidd Creek berthierine and those samples listed in Table 2 from Corby (England), Hiramatsu (Japan), and the USSR (not plotted), all are more aluminous than the Kidd Creek chlorite. Note that in deformed sample KC-2505 (Fig. 2F), the microprobe data reported in Table 2 for the berthierine lamellae (2505F-2) also indicate a more aluminous composition than that of the coexisting chlorite (2505F-1). With the exception of sample 2505, this probably is unrelated to the extent of octahedral-site vacancies, which span a similar range in the berthierine (Table 2) and chlorite (Slack & Coad 1989, Table 2).

## DISCUSSION

Berthierine is a common mineral in many Fe-rich sedimentary rocks, especially ironstones and iron formations (e.g., French 1973, Bhattacharyya 1983, Van Houten & Purucker 1984, Maynard 1986). Recent mineralogical studies also have identified berthierine in

soils and bauxites (Kodama & Foscolos 1981, Nikitina 1985), unmetamorphosed coal measures of Japan (Iijima & Matsumoto 1982), diagenetically altered clastic sediments of the Gulf Coast (Ahn & Peacor 1985), clastic reservoirs of offshore Norway (Jahren & Aagaard 1989), conglomerates from England (Taylor 1990), and some low-grade pelitic schists from Venezuela and Spain (Amouric *et al.* 1988, Bons & Schryvers 1989). Documented occurrences of berthierine in hydrothermal settings are less extensive, and mainly involve sulfide-bearing veins such as in France (Caillère & Hénin 1956), Czechoslovakia (Novak *et al.* 1959), England (Smith & Hardy 1981), the former Soviet Union (Rusinova *et al.* 1987), and Niger (Perez *et al.* 1990); berthierine also has been reported recently from hydrothermally altered shales in the Salton Sea geothermal field of California (Yau *et al.* 1988, Walker & Thompson 1990). The berthierine identified from the Kidd Creek mine in this study represents the first known occurrence in submarine massive sulfide environments.

#### *Formation of berthierine*

Possible mechanisms for the formation of the Kidd Creek berthierine involve hydrothermal, metamorphic, and postmetamorphic processes. Interpretations of pre-metamorphic hydrothermal growth are based on the presence of large prismatic crystals in pristine sample KC-3421 (Fig. 2C), and on equilibrium textures observed in relatively undeformed samples such as KC-813 (Fig. 2D) that are similar to those observed in modern sulfide deposits from the sea floor (*e.g.*, Alt *et al.* 1987, Alt & Jiang 1991), where mineral grains commonly are euhedral and form straight contacts with layer silicates, presumably as a result of crystallization in a stress-free environment.

Experimental studies also are consistent with a hydrothermal origin for some of the Kidd Creek berthierine. All of the synthesis work done to date on chlorite has made 7 Å, not 14 Å phases, as initial run products (*e.g.*, Nelson & Roy 1958, Turnock 1960). In a detailed study of the stability of iron-rich chlorite, James *et al.* (1976) synthesized 7 Å Fe-rich silicate at 300°C and 2 kbar P(H<sub>2</sub>O), whereas crystallization of 14 Å Fe-rich chlorite required longer run times (six weeks) at temperatures in excess of 525°C. More recently, Nikol'skaia *et al.* (1985) formed berthierine by reacting kaolinite with FeCl<sub>3</sub> at 400°C, and Yau *et al.* (1987) synthesized berthierine ± illite at 300°C from an interlayered illite-smectite precursor. These experiments show that berthierine, although probably metastable, may form in hydrothermal systems at relatively high temperatures of 300–400°C. The inferred hydrothermal berthierine from Kidd Creek is believed to have formed under similar temperature conditions (*e.g.*, Slack & Coad 1989). The formation of the hydrothermal berthierine probably occurred by replacement of a pre-existing aluminous phase, rather than by direct precipitation from solution,

based on the low solubility of Al in most hydrothermal solutions and the very low Al/Fe ratios of end-member (Mg-free) compositions calculated for fluids sampled at modern submarine vents (Bowers & Taylor 1985, Von Damm & Bischoff 1987). We cannot exclude the possibility, however, that some of the Kidd Creek berthierine precipitated directly from hydrothermal solutions, like the illite-smectite recently discovered by Alt & Jiang (1991) from massive sulfide deposits on the sea floor.

Textural relations and experimental work (Yau *et al.* 1987) suggest that the initial formation of berthierine may have involved growth from an illite-smectite precursor (*e.g.*, Fig. 2C), or possibly a kaolinite precursor (Bhattacharyya 1983, Nikol'skaia *et al.* 1985) that reacted with Fe-rich hydrothermal fluids. The latter interpretation is considered less likely, on the basis of the observed paragenetic relations among berthierine, muscovite, and halloysite in the Kidd Creek samples. Smectite also is not a favored precursor because of the lack of significant Na or Ca recorded in the microprobe data for the berthierine (Table 2), although Na and Ca could have been leached from smectite during hydrothermal alteration to berthierine. Most, if not all, of the premetamorphic berthierine at Kidd Creek is believed to have formed by the hydrothermal replacement of pre-existing muscovite or chlorite at temperatures of approximately 350°C (Slack & Coad 1989), which produced the observed embayment textures and euhedral pseudomorphs.

Evidence in support of a syn- or postmetamorphic origin for some of the berthierine comes mainly from textural features documented by SEM and TEM studies. These include the lamellar intergrowths observed in deformed sample KC-2505 (Fig. 2F), and the relations between deformed chlorite and undeformed berthierine illustrated in the lattice fringe images of the same sample (Figs. 3, 5). The latter textures are common in intergrown stacks of phyllosilicates that formed as stable coexisting assemblages in low- to medium-grade, greenschist-facies rocks (*e.g.*, Franceschelli *et al.* 1986, Frey 1987, Jiang *et al.* 1990) and in phyllosilicate aggregates that formed through partial replacement of a precursor phase (*e.g.*, Jiang & Peacor 1991). We cannot discriminate between syn- and postmetamorphic growth of this berthierine, but regardless of the timing, it seems likely that it replaced pre-existing chlorite, either of hydrothermal or metamorphic origin. The Fe necessary for the formation of this metamorphic berthierine may have come from the rims of tourmaline crystals in the footwall stringer zone that were leached of substantial amounts of Fe, Ti, and Ca (Slack & Coad 1989, Figs. 5, 11), possibly during the late metasomatic event documented in the mine area by Maas *et al.* (1986). The formation of the Fe-chlorite may have involved alteration of berthierine in the later stages of multiple metamorphic events in the region, identified by Brisbin *et al.* (1990) and Barrie & Davis (1990).

### Preservation of hydrothermal berthierine

Berthierine is generally considered to be a metastable phase that inverts to 14 Å Fe-rich chlorite during diagenesis and metamorphism. In clastic sediments, berthierine is preferentially found at shallow depths relative to Fe-rich chlorite, which commonly is coarser grained and paragenetically later than the associated berthierine (Frey 1970, 1978, Lee & Peacor 1983, Ahn & Peacor 1985). Velde *et al.* (1974) suggested that in arenites and calcarenites, 7 Å berthierine undergoes a polymorphic transformation to 14 Å chlorite at temperatures of 25–100°C. Similar relations are observed in hydrothermally altered sediments from the Salton Sea geothermal field, where berthierine is found in shallow, low-temperature settings relative to the deeper, higher temperature occurrences of Fe-rich chlorite (Yau *et al.* 1988, Walker & Thompson 1990).

The presence in sample KC-3421 of large (100–200 µm) prismatic crystals of berthierine together with halloysite (Figs. 2A, B), a likely metastable precursor to kaolinite (Churchman & Carr 1975, Steefel & Van Cappellen 1990), suggests that this Kidd Creek berthierine is a primary hydrothermal phase and that the halloysite formed by late hydrothermal processes, as discussed above. The preservation of berthierine and halloysite in this sample may reflect the armoring of layer silicates by massive sulfide, thus preventing interaction with metamorphic fluids that would have converted these silicates to Fe-rich chlorite and kaolinite (or illite), respectively. This interpretation is supported by the fact that samples containing tourmaline with a metamorphic reaction-rim (Slack & Coad 1989) have chlorite but little or no berthierine, whereas tourmaline crystals in other samples that contain abundant berthierine (*e.g.*, KC-813) show little or no evidence for interaction with a metamorphic fluid (*i.e.*, absence of a reaction rim).

### Evolution of the Kidd Creek stringer zone

Many electron-microprobe studies have shown that massive sulfide deposits are dominated by Mg-rich chlorite, but that some deposits contain local Fe-rich chlorite [ $Fe/(Fe+Mg) > 0.8$ ], as summarized by Urabe *et al.* (1983) and Slack & Coad (1989). The inner cores of footwall zones of alteration in the deposits may show preferential concentration of either Mg- or Fe-rich chlorite, relative to peripheral zones (*e.g.*, Franklin *et al.* 1981, Urabe *et al.* 1983, Gustin 1990). Such compositional variations in chlorite chemistry are generally attributed to precipitation from solutions containing variable proportions of Mg-rich seawater and Fe-rich hydrothermal fluid (Roberts & Reardon 1978, Zierenberg *et al.* 1988). The compositional variations of the Kidd Creek chlorite were interpreted by Slack & Coad (1989) in a similar manner: the Fe–Mg chlorite formed first and was overprinted or replaced by Fe-rich “chlo-

rite” (*i.e.*, berthierine) where alteration and mineralization associated with an earlier hydrothermal event were believed to have sealed off the footwall zone of alteration from infiltration by Mg-rich seawater. The recognition of berthierine in the deposit, however, requires a re-evaluation of this interpretation.

Slack & Coad (1989) proposed the existence of two hydrothermal events in the Kidd Creek deposit, in which early formation of Fe–Mg chlorite and tourmaline was followed by a second event that chemically overprinted the chlorite to form daphnite (*i.e.*, berthierine), whereas the compositions of the chemically more resistant tourmaline remained unaffected. However, the SEM and TEM observations of complex berthierine–chlorite intergrowths suggest instead that most of the 7 Å berthierine formed first from an Fe-rich, end-member hydrothermal fluid and that the 14 Å Fe–Mg chlorite formed later from a seawater-dominated fluid; quartz, tourmaline, and sulfides apparently were precipitated during both events of fluid circulation. These mineralizing events need not have been separated by a significant time interval, however, and could have been part of one long-lived seafloor hydrothermal system. The apparent disequilibrium between the Fe/(Fe+Mg) ratios of chlorites and tourmaline rims suggested by Slack & Coad (1989) therefore may not indicate the presence of two unrelated hydrothermal fluids in the footwall stringer zone, but instead could reflect the occurrence of berthierine (rather than daphnite) in samples with Fe/(Fe+Mg) ratios that fall off the equilibrium  $K_D$  curves for chlorite and tourmaline (see Slack & Coad 1989, Fig. 13).

### Implications for modern and ancient volcanogenic massive sulfide deposits

The recognition of berthierine in the Archean Kidd Creek massive sulfide deposit has implications for similar ancient, as well as modern, volcanogenic sulfide deposits. Particularly interesting are the calculated stability-relations of berthierine relative to other Fe–Al silicates (Fig. 9). This diagram was constructed for a temperature of 350°C under conditions of quartz saturation using thermodynamic data from SUPCRT (see Bowers *et al.* 1984, and references therein), except the free energy and enthalpy data for daphnite (14 Å) and berthierine (“7 Å chamosite”), which are from Wolery (1978, Table 2). Despite uncertainties in the thermodynamic data, the calculations show that berthierine has a similar, but smaller field of stability relative to that of daphnite (14 Å Fe-rich chlorite), and therefore probably is metastable. Based on textural relations (*e.g.*, Fig. 2D), the Kidd Creek berthierine and muscovite appear to be coeval and may have formed under equilibrium conditions in some of the samples, in agreement with the thermodynamic relations. In a recent study of Ag–Pb–Zn polymetallic veins in the Ukraine, Rusinova *et al.* (1987) determined that berthierine formed simultaneously with sericite and K-feldspar. The apparent theo-

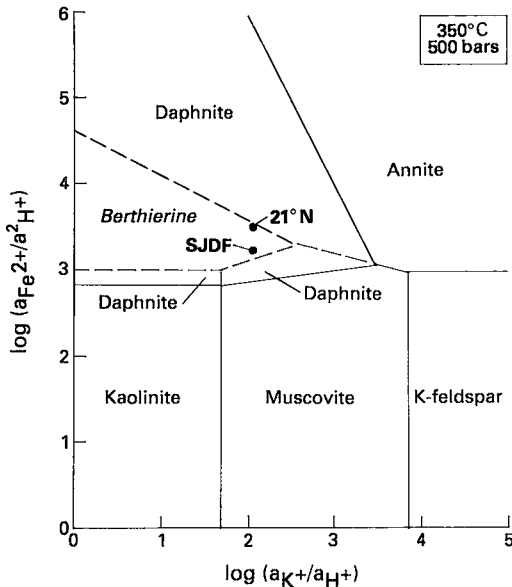


Fig. 9. Activity diagram showing stability relations of minerals in the system  $\text{FeO}-\text{K}_2\text{O}-\text{Al}_2\text{O}_3-\text{SiO}_2-\text{H}_2\text{O}$  at  $350^\circ\text{C}$  and 500 bars. Activities of minerals and  $\text{H}_2\text{O}$  are set at 1.0 under conditions of quartz saturation. Thermodynamic data and calculations from SUPCRT (see Bowers *et al.* 1984, and references therein) except free energy and enthalpy data for daphnite (14 Å) and berthierine ("7 Å chamosite"), which are from Wolery (1978, Table 2). Data points for end-member vent fluids from  $21^\circ\text{N}$  (OBS) and the southern Juan de Fuca Ridge (Plume) were calculated by J.K. Böhlke (USGS) using the program SOLVEQ (Reed 1982, Spycher & Reed 1989) and the fluid compositions reported by Von Damm *et al.* (1985) and Von Damm & Bischoff (1987), respectively. Note smaller field of stability of berthierine (dashed) relative to that of daphnite.

retical incompatibility of this assemblage (Fig. 9) may be an artifact of the thermodynamic data-base, however, particularly the position of the K-feldspar – muscovite – quartz buffer, and therefore does not necessarily conflict with the paragenetic observations of Rusinova *et al.* (1987) for the vein deposits they studied.

The thermodynamic data also permit an evaluation of the stability of Fe-silicates in modern submarine hydrothermal systems. Calculated compositions of end-member vent fluids at  $350^\circ\text{C}$  from the OBS site at  $21^\circ\text{N}$  on the East Pacific Rise and from the Plume site on the southern Juan de Fuca Ridge are both within the stability field of berthierine (Fig. 9). Such relations suggest that metastable berthierine may be currently forming in the subsurface feeder zones of these active submarine hydrothermal vents. Additional candidates include the

Galapagos Ridge (Embley *et al.* 1988) and the Kane Fracture Zone of the Mid-Atlantic Ridge (Delaney *et al.* 1987), where reported Fe-rich chlorite likely contains minor to major amounts of berthierine.

The difficulty of identifying berthierine by routine optical, X-ray, and electron-microprobe methods suggests that much of the Fe-rich chlorite reported from modern and ancient massive sulfide deposits may instead be berthierine. Recognition of premetamorphic berthierine in such deposits is important because it records the preservation of primary mineral assemblages deposited by paragenetically early, Fe-rich hydrothermal fluids. Additional mineralogical studies integrating SEM, TEM, and electron-microprobe data are needed on layer silicates from other unmetamorphosed or weakly metamorphosed massive sulfide deposits on land, and from modern deposits on the sea floor. Such studies will be useful for accurately documenting mineral compositions and paragenetic relations in alteration zones related to massive sulfide deposits, and for improving our understanding of fluid-rock reactions in submarine hydrothermal systems.

#### ACKNOWLEDGEMENTS

The senior author thanks L.T. Bryndzia for urging X-ray verification of the Kidd Creek "daphnite", which provided the basis for this study. We also thank the late J.W. Hosterman for acquiring the XRD data, C.A. Consolvo for help in sample preparation, and J.V. Emery and J.J. McGee for SEM imaging. We are grateful to H.T. Evans, Jr., for the identification of the halloysite, and to J.K. Böhlke for assistance with thermodynamic calculations. Translations of Russian articles were kindly supplied by N. Tamberg. We thank G.R. Robinson, Jr. and J.K. Böhlke for comments on an early version of the manuscript, and Jung-Ho Ahn and J.E. Chisholm for journal reviews. The scanning transmission electron microscope used in this study was acquired under grant EAR-87-08276 from the National Science Foundation, and was partially supported by NSF grants EAR-88-17080 and EAR-86-04170 to D.R. Peacor. We also acknowledge the staff and management of Kidd Creek Mines and Falconbridge Limited for providing underground access and drill core for study.

#### REFERENCES

- AHN, JUNG-HO & PEACOR, D.R. (1985): Transmission electron microscopic study of diagenetic chlorite in Gulf Coast argillaceous sediments. *Clays Clay Minerals* **33**, 228-236.
- \_\_\_\_\_ & \_\_\_\_\_ (1987): Kaolinization of biotite: TEM data and implications for an alteration mechanism. *Am. Mineral.* **72**, 353-356.
- ALBEE, A.L. (1962): Relationships between the mineral association, chemical composition and physical properties of the chlorite series. *Am. Mineral.* **47**, 851-870.

- ALT, J.C. & JIANG, WEI-TEH (1991): Hydrothermally precipitated mixed-layer illite-smectite in recent massive sulfide deposits from the sea floor. *Geology* **19**, 570-573.
- \_\_\_\_\_, LONSDALE, P., HAYMON, R. & MUEHLENBACHS, K. (1987): Hydrothermal sulfide and oxide deposits on seamounts near 21°N, East Pacific Rise. *Geol. Soc. Am. Bull.* **98**, 157-168.
- AMOURIC, M., GIANETTO, I. & PROUST, D. (1988): 7, 10, and 14 Å mixed-layer phyllosilicates studied structurally by TEM in pelitic rocks of the Piemontese zone (Venezuela). *Bull. Minéral.* **111**, 29-37.
- BAILEY, S.W. (1988): Structures and compositions of other trioctahedral 1:1 phyllosilicates. In *Hydrous Phyllosilicates (Exclusive of Micas)* (S.W. Bailey, ed.). *Rev. Mineral.* **19**, 169-188.
- \_\_\_\_\_, & LISTER, J.S. (1989): Structures, compositions, and x-ray diffraction identification of dioctahedral chlorites. *Clays Clay Minerals* **37**, 193-202.
- BANFIELD, J.F. & EGGLETON, R.A. (1988): Transmission electron microscope study of biotite weathering. *Clays Clay Minerals* **36**, 47-60.
- BARRIE, C.T. & DAVIS, D.W. (1990): Timing of magmatism and deformation in the Kamiskotia – Kidd Creek area, western Abitibi Subprovince, Canada. *Precambrian Res.* **46**, 217-240.
- BHATTACHARYYA, D.P. (1983): Origin of berthierine in ironstones. *Clays Clay Minerals* **31**, 173-182.
- BONS, A.-J. (1988): Deformation of chlorite in naturally deformed low-grade rocks. *Tectonophysics* **154**, 149-165.
- \_\_\_\_\_, DRURY, M.R., SCHRYVERS, D. & ZWART, H.J. (1990): The nature of grain boundaries in slates. Implications for mass transport processes during low temperature metamorphism. *Phys. Chem. Minerals* **17**, 402-408.
- \_\_\_\_\_, & SCHRYVERS, D. (1989): High-resolution electron microscopy of stacking irregularities in chlorites from the central Pyrenees. *Am. Mineral.* **74**, 1113-1123.
- BOWERS, T.S., JACKSON, K.L. & HELGESON, H.C. (1984): *Equilibrium Activity Diagrams for Coexisting Minerals and Aqueous Solutions at Pressures and Temperatures to 5 kb and 600°C*. Springer-Verlag, Berlin.
- \_\_\_\_\_, & TAYLOR, H.P., JR. (1985): An integrated chemical and stable-isotope model of the origin of mid-ocean ridge hot spring systems. *J. Geophys. Res.* **90**, 12,583-12,606.
- BRINDLEY, G.W. (1951): The crystal structure of some chamosite minerals. *Mineral. Mag.* **29**, 502-525.
- \_\_\_\_\_, (1982): Chemical compositions of berthierines – a review. *Clays Clay Minerals* **30**, 153-155.
- \_\_\_\_\_, & YUELL, R.F. (1953): Ferrous chamosite and ferric chamosite. *Mineral. Mag.* **30**, 57-70.
- BRISBIN, D., KELLY, V. & COOK, R. (1990): Kidd Creek mine. In *Geology and Ore Deposits of the Timmins District, Ontario* (J.A. Fyon & A.H. Green, eds.). *Eighth IAGOD Symp., Field Trip Guidebook 6; Geol. Surv. Can., Open-File Rep.* **2161**, 66-76.
- CAILLÈRE, S. & HÉNIN, M.S. (1956): Sur la présence de la berthierine dans une diaclase du gisement de Diélette. *C.R. Congrès Soc. Savantes Paris* **81**, 5-8.
- CHURCHMAN, G.J. & CARR, R.M. (1975): The definition and nomenclature of halloysites. *Clays Clay Minerals* **23**, 382-388.
- COAD, P.R. (1985): Rhyolite geology at Kidd Creek – a progress report. *Can. Inst. Mining Metall. Bull.* **78**(874), 70-83.
- CRAIG, J., FITCHES, W.R. & MALTMAN, A.J. (1982): Chlorite-mica stacks in low-strain rocks from central Wales. *Geol. Mag.* **119**, 243-256.
- CURTIS, C.D., HUGHES, C.R., WHITEMAN, J.A. & WHITTLE, C.K. (1985): Compositional variations within some sedimentary chlorites and some comments on their origin. *Mineral. Mag.* **49**, 375-386.
- DEAN, R.S. (1983): Authigenic trioctahedral clay minerals coating Clearwater Formation sand grains at Cold Lake, Alberta, Canada. *20th Ann. Mtg., Clay Mineral. Soc.*, 79 (abstr.).
- DELANEY, J.R., MOGK, D.W. & MOTTI, M.J. (1987): Quartz-cemented breccias from the Mid-Atlantic Ridge: samples of a high-salinity hydrothermal upflow zone. *J. Geophys. Res.* **92**, 9175-9192.
- EMBLEY, R.W., JONASSON, I.R., PERFIT, M.R., FRANKLIN, J.M., TIVEY, M.A., MALAHOFF, A., SMITH, M.F. & FRANCIS, T.J.G. (1988): Submersible investigation of an extinct hydrothermal system on the Galapagos Ridge: sulfide mounds, stockwork zone, and differentiated lavas. *Can. Mineral.* **26**, 517-539.
- FOSTER, M.D. (1962): Interpretation of the composition and a classification of the chlorites. *U.S. Geol. Surv., Prof. Pap.* **414A**, 1-33.
- FRANCESCHELLI, M., MELLINI, M., MEMMI, I. & RICCI, C.A. (1986): Fine-scale chlorite-muscovite association in low-grade metapelites from Nurra (NW Sardinia), and the possible misidentification of metamorphic vermiculite. *Contrib. Mineral. Petrol.* **93**, 137-143.
- FRANKLIN, J.M., LYDON, J.W. & SANGSTER, D.F. (1981): Volcanic-associated massive sulfide deposits. *Econ. Geol., 75th Ann. Vol.* 485-627.
- FRANSOLET, A.-M. & BOURGUIGNON, P. (1975): Données nouvelles sur la fraipontite de Moresnet (Belgique). *Bull. Soc. Franç. Minéral. Cristallogr.* **98**, 235-244.
- FRENCH, B.M. (1973): Mineral assemblages in diagenetic and low-grade metamorphic iron-formation. *Econ. Geol.* **68**, 1063-1074.

- FREY, M. (1970): The step from diagenesis to metamorphism in pelitic rocks during Alpine orogenesis. *Sedimentol.* **15**, 261-279.
- (1978): Progressive low-grade metamorphism of a black shale formation, central Swiss Alps, with special reference to pyrophyllite and margarite bearing assemblages. *J. Petrol.* **19**, 95-135.
- (1987): The reaction-isograd kaolinite + quartz = pyrophyllite + H<sub>2</sub>O, Helvetic Alps, Switzerland. *Schweiz. Mineral. Petrogr. Mitt.* **67**, 1-11.
- GREGG, W.J. (1986): Deformation of chlorite-mica aggregates in cleaved psammitic and pelitic rocks from Islesboro, Maine, U.S.A. *J. Struct. Geol.* **8**, 59-68.
- GUSTIN, M.S. (1990): Stratigraphy and alteration of the host rocks, United Verde massive sulfide deposit, Jerome, Arizona. *Econ. Geol.* **85**, 29-49.
- HAYASHI, H. & OINUMA, K. (1964): Aluminian chlorite from Kamikita mine, Japan. *Clay Sci.* **2**, 22-30.
- HEY, M.H. (1954): A new review of the chlorites. *Mineral. Mag.* **30**, 277-292.
- IJIMA, A. (1974): Clay and zeolitic alteration zones surrounding Kuroko deposits in the Hokuroku district, northern Akita, as submarine hydrothermal-diagenetic alteration products. *Mining Geol., Spec. Issue* **6**, 267-289.
- & MATSUMOTO, R. (1982): Berthierine and chamosite in coal measures of Japan. *Clays Clay Minerals* **30**, 264-274.
- JAHREN, J.S. & AAGAARD, P. (1989): Compositional variations in diagenetic chlorites and illites, and relationships with formation-water chemistry. *Clay Minerals* **24**, 157-170.
- JAMES, R.S., TURNOCK, A.C. & FAWCETT, J.J. (1976): The stability and phase relations of iron chlorite below 8.5 kb P<sub>H2O</sub>. *Contrib. Mineral. Petrol.* **56**, 1-25.
- JIANG, WEI-TEH, ESSENE, E.J. & PEACOR, D.R. (1990): Transmission electron microscopic study of coexisting pyrophyllite and muscovite: direct evidence for the metastability of illite. *Clays Clay Minerals* **38**, 225-240.
- & PEACOR, D.R. (1991): Transmission electron microscopic study of the kaolinitization of muscovite. *Clays Clay Minerals* **39**, 1-13.
- KISCH, H.J. (1983): Mineralogy and petrology of burial diagenesis (burial metamorphism) and incipient metamorphism in clastic rocks. In *Diagenesis in Sediments and Sedimentary Rocks*, 2 (G. Larsen & G.V. Chilingar, eds.). Elsevier, New York (289-493).
- (1987): Correlation between indicators of very low-grade metamorphism. In *Low Temperature Metamorphism* (M. Frey, ed.). Chapman and Hall, New York (227-300).
- KODAMA, H. & FOSCOLOS, A.E. (1981): Occurrence of berthierine in Canadian Arctic desert soils. *Can. Mineral.* **19**, 279-283.
- LEE, J.H. & PEACOR, D.R. (1983): Interlayer transitions in phyllosilicates of Martinsburg Shale. *Nature* **303**, 608-609.
- LYDON, J.W. & GALLEY, A. (1986): Chemical and mineralogical zonation of the Mathiati alteration pipe, Cyprus, and its genetic significance. In *Metallogeny of Basic and Ultrabasic Rocks* (M.J. Gallagher, R.A. Ixer, C.R. Neary & H.M. Prichard, eds.). The Institution of Mining and Metallurgy, London (49-68).
- MAAS, R., MCCULLOCH, M.T., CAMPBELL, I.H. & COAD, P.R. (1986): Sm-Nd and Rb-Sr dating of an Archean massive sulfide deposit: Kidd Creek, Ontario. *Geology* **14**, 585-588.
- MARUMO, K. (1991): A comparison of mineral assemblages in the alteration haloes of the Middle Miocene Kuroko deposits in Japan and their modern analogue (Jade) in the backarc Okinawa Trough. *Geol. Assoc. Can. - Mineral. Assoc. Can., Program. Abstr.* **16**, A80.
- MAYNARD, J.B. (1986): Geochemistry of oolitic iron ores, an electron microprobe study. *Econ. Geol.* **81**, 1473-1483.
- NELSON, B.W. & ROY, R. (1958): Synthesis of the chlorites and their structural and chemical constitution. *Am. Mineral.* **43**, 707-725.
- NIKITINA, A.P. (1985): Distribution and genesis of clay minerals and free alumina minerals in the deposits of residual bauxites in the European part of the USSR. In *Proc. 5th Meet., European Clay Groups* (J. Konta, ed.). Charles University, Prague (351-357).
- NIKOL'SKAIA, N.K., KOTOV, N.V., FRANK-KAMENETSKII, V.A. & GOILO, E.A. (1985): Hydrothermal transformations of kaolinite in iron-bearing media at elevated P<sub>H2O</sub>-T parameters. *Vestnik Leningrad Univ. Geol. Geogr.* **14**, 8-14 (in Russ.).
- NOVAK, F., VTELENSKY, J., LOSERT, J., KUPKA, F. & VALCHA, Z. (1959): Orthochamosit, ein neues Mineral aus den hydrothermalen Erzgängen von Kank bei Kutná Hora (Kuttenberg) in der Tschechoslowakei. *Geologie* **8**(2), 159-167.
- NUNES, P.D. & PYKE, D.R. (1981): Time-stratigraphic correlation of the Kidd Creek orebody with volcanic rocks south of Timmins, Ontario, as inferred from zircon U-Pb ages. *Econ. Geol.* **76**, 944-951.
- PERCIVAL, J.A. & KROGH, T.E. (1983): U-Pb zircon geochronology of the Kapuskasing structural zone and vicinity in the Chappleau-Foley area, Ontario. *Can. J. Earth Sci.* **20**, 830-843.
- PEREZ, J.-B., DUSAUSOY, Y., BABKINE, J. & PAGEL, M. (1990): Mn zonation and fluid inclusions in genthelvite from the Taghouaji complex (Air Mountains, Niger). *Am. Mineral.* **75**, 909-914.
- REED, M.H. (1982): Calculation of multicomponent chemical

- equilibria and reaction processes in systems involving minerals, gases and an aqueous phase. *Geochim. Cosmochim. Acta* **46**, 513-528.
- REYNOLDS, R.C., JR. (1988): Mixed layer chlorite minerals. In *Hydrous Phyllosilicates (Exclusive of Micas)* (S.W. Bailey, ed.). *Rev. Mineral.* **15**, 601-629.
- RICHARDS, H.G., CANN, J.R. & JENSENIUS, J. (1989): Mineralogical zoning and metasomatism of the alteration pipes of Cyprus sulfide deposits. *Econ. Geol.* **84**, 91-115.
- ROBERTS, R.G. & REARDON, E.J. (1978): Alteration and ore-forming processes at Mattagami Lake mine, Quebec. *Can. J. Earth Sci.* **15**, 1-21.
- RUSINOVA, O.V., KOBTSEV, B.M., FEDOSOVA, S.P. & GURENKO, O.YU. (1987): Berthierine-chlorite mixtures in hydrothermal deposits. *Bull. Mosk. Obshchest. Pridody, Otd. Geol.* **62**, 100-105 (in Russ.).
- SHAU, YEN-HONG, PEACOR, D.R. & ESSENE, E.J. (1990): Corrensite and mixed-layer chlorite/corrensite in metabasalt from northern Taiwan: TEM/AEM, EPMA, XRD, and optical studies. *Contrib. Mineral. Petrol.* **105**, 123-142.
- SHIROZU, H. (1974): Clay minerals in altered wall rocks of the Kuroko-type deposits. *Mining Geol., Spec. Issue* **6**, 303-310.
- \_\_\_\_\_, SAKASEGAWA, T., KATSUMOTO, N. & OZAKI, M. (1975): Mg-chlorite and interstratified Mg-chlorite/saponite associated with Kuroko deposits. *Clay Sci.* **4**, 305-321.
- SLACK, J.F. & COAD, P.R. (1989): Multiple hydrothermal and metamorphic events in the Kidd Creek volcanogenic massive sulphide deposit, Timmins, Ontario: evidence from tourmalines and chlorites. *Can. J. Earth Sci.* **26**, 694-715.
- SMITH, F.W. & HARDY, R.G. (1981): Clay minerals in the veins of the North Pennine orefield, UK. *Clay Minerals* **16**, 309-312.
- SPYCHER, N.F. & REED, M.H. (1989): *SOLVEQ: a Computer Program for Computing Aqueous-Mineral-Gas Equilibria*. Dep. Geological Sci., Univ. Oregon, Eugene, Oregon.
- STANTON, R.L. (1983): The direct derivation of sillimanite from a kaolinitic precursor: evidence from the Geco mine, Manitouwadge, Ontario. *Econ. Geol.* **78**, 422-437.
- \_\_\_\_\_. (1984): The direct derivation of cordierite from a clay-chlorite precursor: evidence from the Geco mine, Manitouwadge, Ontario. *Econ. Geol.* **79**, 1245-1264.
- STEEFEL, C.I. & VAN CAPPELLEN, P. (1990): A new kinetic approach to modeling water-rock interaction: the role of nucleation, precursors, and Ostwald ripening. *Geochim. Cosmochim. Acta* **54**, 2657-2677.
- TAYLOR, K.G. (1990): Berthierine from the non-marine Wealch to modeling - den (Early Cretaceous) sediments of south-east England. *Clay Minerals* **25**, 391-399.
- TSUKAHARA, N. (1964): Dioctahedral chlorite from the Furu-tobe mine, Akita Prefecture, Japan. *Clay Sci.* **2**, 56-75.
- TURNOCK, A.C. (1960): The stability of iron chlorites. *Carnegie Inst. Wash., Yearbook* **59**, 98-103.
- URABE, T., SCOTT, S.D. & HATTORI, K. (1983): A comparison of footwall-rock alteration and geothermal systems beneath some Japanese and Canadian volcanogenic massive sulfide deposits. *Econ. Geol., Monogr.* **5**, 345-364.
- UTADA, M., MINATO, H., ISHIKAWA, T. & YOSHIZAKI, Y. (1974): The alteration zones surrounding Kuroko-type deposits in Nishi-Aizu district, Fukushima Prefecture, with emphasis on the analcime zone as an indicator in exploration for ore deposits. *Mining Geol., Spec. Issue* **6**, 291-302.
- VAN DER PLUIJM, B.A. & KAARS-SUPESTEIJN, C.H. (1984): Chlorite-mica aggregates: morphology, orientation, development and bearing on cleavage formation in very low-grade rocks. *J. Struct. Geol.* **6**, 399-407.
- VAN HOUTEN, F.B. & PURUCKER, M.E. (1984): Glauconite peloids and chamositic ooids - favorable factors, constraints and problems. *Earth Sci. Rev.* **20**, 211-243.
- VELDE, B. (1973): Phase equilibria in the system MgO-Al<sub>2</sub>O<sub>3</sub>-SiO<sub>2</sub>-H<sub>2</sub>O: chlorites and associated minerals. *Mineral. Mag.* **39**, 297-312.
- \_\_\_\_\_. (1989): Phyllosilicate formation in berthierine peloids and iron oolites. In *Phanerozoic Ironstones* (T.P. Young & W.E.G. Taylor, eds.). *Geol. Soc. London, Spec. Publ.* **46**, 3-8.
- \_\_\_\_\_, RAOULT, J.F. & LEIKINE, M. (1974): Metamorphosed berthierine pellets in Mid-Cretaceous rocks from north-eastern Algeria. *J. Sed. Petrol.* **44**, 1275-1280.
- VON DAMM, K.L. & BISCHOFF, J.L. (1987): Chemistry of hydrothermal solutions from the southern Juan de Fuca Ridge. *J. Geophys. Res.* **92**, 11,334-11,346.
- \_\_\_\_\_, EDMOND, J.M., GRANT, B., MEASURES, C.I., WALDEN, B. & WEISS, R.F. (1985): Chemistry of submarine hydrothermal solutions at 21°N, East Pacific Rise. *Geochim. Cosmochim. Acta* **49**, 2197-2220.
- WALKER, J.R. & THOMPSON, G.R. (1990): Structural variations in chlorite and illite in a diagenetic sequence from the Imperial Valley, California. *Clays Clay Minerals* **38**, 315-321.
- WALKER, R.R., MATULICH, A., AMOS, A.C., WATKINS, J.J. & MANNARD, G.W. (1975): The geology of the Kidd Creek mine. *Econ. Geol.* **70**, 80-89.
- WOLERY, T.J. (1978): *Some Chemical Aspects of Hydrothermal Processes at Mid-Oceanic Ridges - A Theoretical Study. I. Basalt - Sea Water Reaction and Chemical Cycling Between the Oceanic Crust and the Oceans. II. Calculation of Chemical Equilibrium Between Aqueous Solutions and Minerals*. Ph.D. thesis, Northwestern Univ., Evanston, Illinois.

- YAU, YU-CHYI, PEACOR, D.R., BEANE, R.E., ESSENE, E.J. & MCDOWELL, S.D. (1988): Microstructures, formation mechanisms, and depth-zoning of phyllosilicates in geothermally altered shales, Salton Sea, California. *Clays Clay Minerals* **36**, 1-10.
- , ———, ESSENE, E.J., LEE, JUNG HOO, KUO, LUNG-CHUAN & COSCA, M.A. (1987): Hydrothermal treatment of smectite, illite, and basalt to 460°C: comparison of natural with hydrothermally formed clay minerals. *Clays Clay Minerals* **35**, 241-250.
- YERSHOVA, Z.P., NIKITINA, A.P., PERFIL'EV, Y.D. & BABESH-KIN, A.M. (1976): Study of chamosites by gamma-resonance (Mössbauer) spectroscopy. *In Proc. Int. Clay Conf., Mexico City, 1975* (S.W. Bailey, ed.). Applied Publishing, Wilmette, Illinois (211-219).
- ZIERENBERG, R.A., SHANKS, W.C., III, SEYFRIED, W.E., JR., KOSKI, R.A. & STRICKLER, M.D. (1988): Mineralization, alteration, and hydrothermal metamorphism of the ophiolite-hosted Turner-Albright sulfide deposit, southwestern Oregon. *J. Geophys. Res.* **93**, 4657-4674.

*Received August 7, 1991, revised manuscript accepted February 25, 1992.*